

High resolution study of the Λp final state interaction in the reaction $p + p \rightarrow K^+ + (\Lambda p)$

The HIRES Collaboration: A. Budzanowski^h, A. Chatterjee^j,
 H. Clement^m, E. Dorochkevitch^m, P. Hawranekⁱ,
 F. Hinterberger^a, R. Jahn^a, R. Joosten^a, K. Kilian^{d,e},
 S. Kliczewski^h, Da. Kirillov^{d,e,c}, Di. Kirillov^b, D. Kolev^k,
 M. Kravcikova^f, M. Lesiak^{i,d,e}, H. Machner^{d,e,c}, A. Magieraⁱ,
 G. Martinska^g, N. Piskunov^b, J. Ritman^{d,e}, P. von Rossen^{d,e},
 B. J. Roy^j, A. Sibirtsev^{a,e}, I. Sitnik^b, R. Siudak^{h,a},
 R. Tsenov^k, K. Ulbrich^a, J. Urban^g, G. J. Wagner^m

^a*Helmholtz-Institut für Strahlen- und Kernphysik, Universität Bonn, Bonn, Germany*

^b*Laboratory for High Energies, JINR Dubna, Russia*

^c*Fachbereich Physik, Universität Duisburg-Essen, Duisburg, Germany*

^d*Institut für Kernphysik, Forschungszentrum Jülich, Jülich, Germany*

^e*Jülich Centre for Hadron Physics, Forschungszentrum Jülich, Jülich, Germany*

^f*Technical University Kosice, Kosice, Slovakia*

^g*P.J. Safarik University, Kosice, Slovakia*

^h*Institute of Nuclear Physics, Polish Academy of Sciences, Krakow, Poland*

ⁱ*Institute of Physics, Jagellonian University, Krakow, Poland*

^j*Nuclear Physics Division, BARC, Mumbai, India*

^k*Physics Faculty, University of Sofia, Sofia, Bulgaria*

^l*University of Chemical Technology and Metallurgy, Sofia, Bulgaria*

^m*Physikalisches Institut, Universität Tübingen, Germany*

Abstract

The reaction $pp \rightarrow K^+ + (\Lambda p)$ was measured at $T_p = 1.953$ GeV and $\Theta = 0^\circ$ with a high missing mass resolution in order to study the Λp final state interaction. The large final state enhancement near the Λp threshold can be described using the standard Jost-function approach. The singlet and triplet scattering lengths and effective ranges are deduced by fitting simultaneously the Λp invariant mass spectrum and the total cross section data of the free Λp scattering.

Key words: Hyperon-nucleon interactions; Forces in hadronic systems and effective interactions; Nuclear reaction models and methods; Nucleon-induced reactions
PACS: 13.75.Ev, 21.30.Fe, 24.10.-i, 25.40.-h

1 Introduction

The study of the Λp interaction is part of the systematic investigation of the hyperon-nucleon (YN) interaction. The YN interaction is an ideal testing ground for the role of strangeness in low and intermediate energy physics. It is also of great relevance in studies of the $SU(3)_{\text{flavor}}$ symmetry. In addition the YN interaction is needed for studies of hypernuclei. Experimental information on the Λp interaction has been obtained from Λp scattering experiments [1,2], the binding energies of hypernuclei [3,4], and studies of the Λp final state interaction (FSI). The Λp FSI was observed in strangeness transfer reactions $K^- + d \rightarrow \pi^- + (\Lambda p)$ [5] and in reactions with associated strangeness production $\pi^+ + d \rightarrow K^+ + (\Lambda p)$ and $p + p \rightarrow K^+ + (\Lambda p)$ [8,9,10,11,12,13,14,15]. The first high resolution study of the reaction $p + p \rightarrow K^+ + (\Lambda p)$ was performed at Saclay [11] with proton kinetic energies of 2.3 and 2.7 GeV and missing mass resolutions between 2 and 5 MeV depending on the scattering angle. The FSI enhancement close to the Λp threshold was later analyzed [16] in terms of the inverse Jost function and the effective range approximation [17]. Recently a new method based on dispersion theory was developed [18,19] in order to extract the scattering length and the effective range and to estimate the theoretical error.

Theoretical studies of the Λp interaction with the Nijmegen [20] and Jülich [21] meson-exchange models predict the potentials, phase shift parameters and effective range parameters. Recently, the Λp interaction has been studied using the chiral effective field theory [22,23]. Another topic of the Λp FSI is the prediction of a narrow $S=-1$ dibaryon resonance by the cloudy bag model with an invariant mass of 2109 MeV [24].

2 Experiment

The reaction $p + p \rightarrow K^+ + (\Lambda p)$ was measured at 0° using the proton beam from the the cooler synchrotron COSY, the magnetic spectrograph BIG KARL

* Corresponding author

Email address: fh@hiskp.uni-bonn.de (F. Hinterberger).

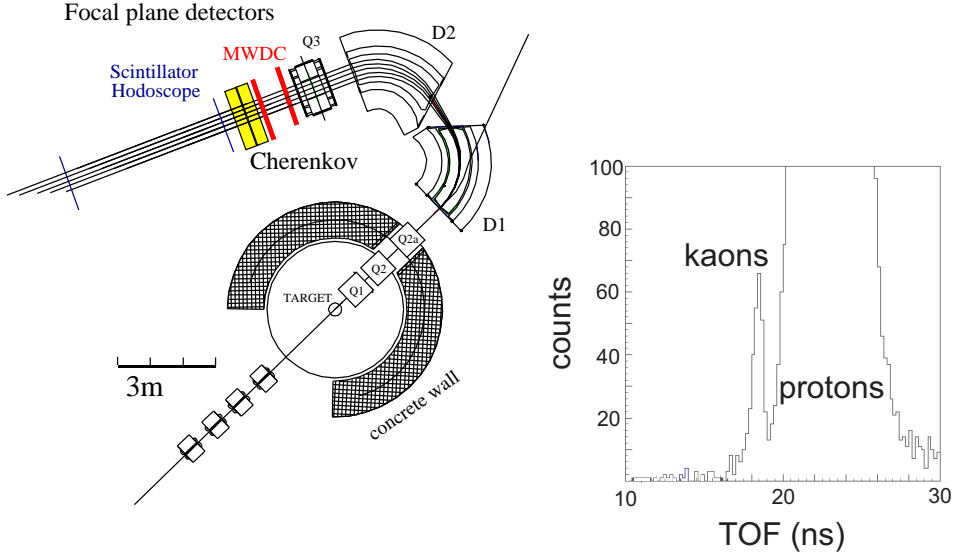


Fig. 1. Left: Layout of the magnetic spectrograph BIG KARL. The charged particle tracks are measured in the focal plane using two stacks of multiwire drift chambers, two threshold Cherenkov detectors and two scintillator hodoscopes. Right: TOF spectrum with pion suppression by two Cherenkov detectors.

[25] and a 1.0 cm thick liquid hydrogen target (see Fig. 1). Since the most important part of the FSI enhancement is located in the sharply rising part near the Λp threshold a high missing-mass resolution was required. The momentum of the incoming proton beam was about 2.735 GeV/c corresponding to a kinetic energy of 1.953 GeV. The absolute beam momentum was found from the fits of the kinematic parameters for two reactions: $p + p \rightarrow K^+ + (\Lambda p)$ and $p + p \rightarrow d + \pi^+$ where kaons and deuterons were measured simultaneously at BIG KARL momentum 1070 MeV/c. The absolute precision of the beam momentum was 0.15 MeV/c. The scattered particles in the momentum range 930 - 1110 MeV/c were detected in the focal plane using two stacks of multiwire drift chambers, two threshold Cherenkov detectors and two scintillator hodoscopes. The ratio of beam momentum to scattered particle momentum was ideally suited for a measurement at 0° . In the first dipole magnet of BIG KARL the beam was magnetically separated from the scattered particles and guided through the side exit of the outer yoke into the beam dump. Thus, the huge background from dumping the beam within the spectrometer has been avoided. Particle identification was performed using the energy loss (ΔE) and time of flight (TOF) information from the scintillator hodoscopes. In addition two threshold Cherenkov detectors [26] were used in order to achieve a very high pion suppression factor of 10^5 . The momentum of the kaon was measured and the missing mass of the Λp system was deduced. The effective missing mass resolution depending on the spread of the beam momentum, the momentum resolution of the magnetic spectrograph and the 1 MeV bin width was $\sigma = 0.84$ MeV. In order to cover the missing mass range 2050 - 2110 MeV three overlapping settings of the spectrograph (mean momenta:

1070, 1010 and 960 MeV/c) were used. The relative precision of the momenta of the three settings was 0.1 MeV/c.

Acceptance corrections with respect to solid angle and momentum were taken from Monte Carlo calculations. The acceptance correction functions contained the magnetic spectrograph momentum acceptance around 0° with (p_x, p_y, p_z) cuts which for a given missing mass bin corresponded to the measured solid angle $d\Omega$. They contained also the detector efficiency corrections. The detector efficiency included efficiency of scintillator detectors which determined trigger and particle identification and magnetic spectrograph efficiency with field inhomogeneity at the edges of the acceptance. Acceptance corrections as determined by Monte Carlo simulations were checked by use of experimental distributions of simultaneously measured pions. They are shown in Fig. 2. The acceptance correction function of the 960 MeV/c setting looks different due to a slightly different (p_x, p_y, p_z) cut.

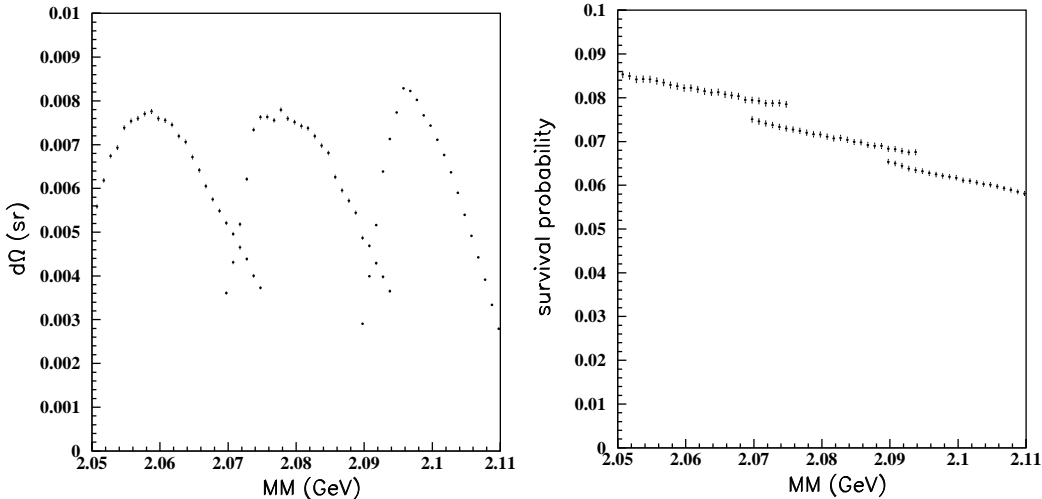


Fig. 2. Left: Acceptance correction functions. Right: Kaon survival probability

The kaon decay along flight path was taken into account for each individual trajectory. Path lengths obtained from calculations of tracks in the magnetic field with the Turtle code [27] were checked by experimentally deduced values from time of flight measurements of pions and protons. The cross section error due to survival probability is less than 1 %. The final kaon survival probability averaged for a given missing mass bin is presented on the right side of Fig. 2.

The relative normalizations of the three different spectrograph settings were deduced from luminosity monitors located in the target area which were independent of the spectrograph settings. The relative normalization errors due to the luminosity measurement were negligibly small. The relative normalization errors due to the acceptance corrections were estimated to be less than 2 %.

The absolute cross section normalization was determined by measuring the

luminosity as described in [25]. At the beginning of each beam period we calibrated two luminosity monitors counting the left and right scattered particles from the target as function of the number of beam particles. To this end, the beam current was highly reduced in order to count the beam particles individually with a fast scintillator hodoscope in the beam dump. For the calibration, the dependence of the luminosity signal on the beam intensity was fitted by a linear function. The resulting beam intensity error amounted to 5 %. The density of the bubble-free liquid hydrogen target ($\rho = 0.0775 \text{ g/cm}^3$) with $1 \mu\text{m}$ thick mylar foil windows was kept constant by stabilizing the temperature to $15.0 \pm 0.5 \text{ K}$ using a high-precision temperature control [28]. The target thickness, i.e. the distance between entrance and exit window (nominal 1 cm) was precisely measured with a calibrated optical telescope. The target thickness error was about 5 %. The overall systematic normalization error was estimated to be 10 %. The missing mass spectrum is shown in Fig. 3.

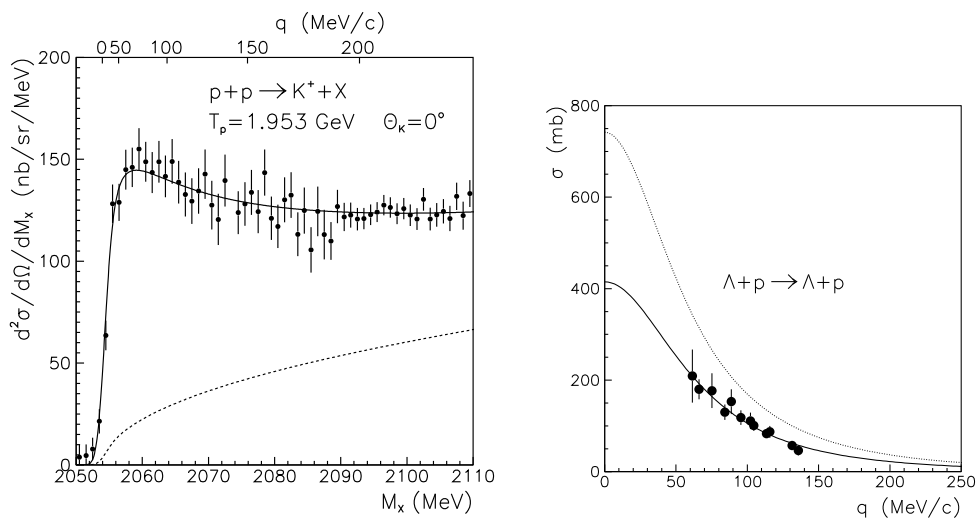


Fig. 3. Left: Missing mass spectrum of the reaction $p + p \rightarrow K^+ + (\Lambda p)$ measured at $T_p = 1.953 \text{ GeV}$ and $\Theta_K = 0^\circ$. The upper axis indicates the c.m. momentum q of the Λp system. Solid line: Combined six-parameter fit. Dashed line: $p + p \rightarrow K^+ + (\Lambda p)$ phase space distribution. The region above 2090 MeV was measured with very small statistical errors in order to study a possible resonance anomaly near 2096.5 and/or 2098.0 MeV [11]. Right: Total $\Lambda p \rightarrow \Lambda p$ cross section [1,2] vs. c.m. momentum q . Solid line: Combined six-parameter fit. Dotted line: Spin-averaged parameters.

3 Formalism

The observed missing mass spectrum can be described by factorizing the reaction amplitude in terms of a production amplitude and a final state enhancement factor. The method of parametrizing the FSI enhancement factor by the inverse Jost function [17] is described in [16]. Taking the spin statistical

weights into account the double differential cross section may be written as

$$\frac{d^2\sigma}{d\Omega_K dM_{\Lambda p}} = \Phi_3 \left[\frac{1}{4} |M_s|^2 \frac{q^2 + \beta_s^2}{q^2 + \alpha_s^2} + \frac{3}{4} |M_t|^2 \frac{q^2 + \beta_t^2}{q^2 + \alpha_t^2} \right]. \quad (3.1)$$

Here, $|M_s|^2$ and $|M_t|^2$ are the singlet and triplet production matrix elements squared, q the internal c.m.-momentum of the Λp system, $\alpha_s, \beta_s, \alpha_t, \beta_t$ the singlet and triplet potential parameters, and Φ_3 the ratio of the three-body phase space distribution¹ and the incident flux factor. The potential parameters α and β can be used to establish phase-equivalent Bargmann potentials [29]. They are related to the scattering lengths a , and effective ranges r of the low-energy S -wave scattering, $\alpha = (1 - \sqrt{1 - 2r/a})/r$, $\beta = (1 + \sqrt{1 - 2r/a})/r$. Instead of the parameters $\alpha_s, \beta_s, \alpha_t$ and β_t one can equally well use the singlet and triplet scattering length and effective range parameters a_s, r_s, a_t and r_t . The expression (3.1) is folded with the Gaussian missing-mass resolution function ($\sigma = 0.84$ MeV) before comparing with the data in the fit program.

The total cross section σ of the free Λp elastic scattering can be expressed at low energies as a function of the c.m.-momentum q using the effective range approximation [17],

$$\sigma = \frac{1}{4} \frac{4\pi}{q^2 + \left(-\frac{1}{a_s} + \frac{r_s q^2}{2}\right)^2} + \frac{3}{4} \frac{4\pi}{q^2 + \left(-\frac{1}{a_t} + \frac{r_t q^2}{2}\right)^2}. \quad (3.2)$$

4 Fit Results

The nonlinear least-square fits are performed using the program Minuit from the CERN library. We determine the spin-averaged scattering length \bar{a} and effective range \bar{r} in a three-parameter fit by applying the constraints $|M_s|^2 = |M_t|^2 = |\bar{M}|^2$, $a_s = a_t = \bar{a}$, $r_s = r_t = \bar{r}$. We fit only the missing mass spectrum without taking the Λp total cross section data into account. The fit yields an excellent description of the missing mass spectrum with $\chi_{red}^2 = 0.55$, $|\bar{M}|^2 = 27.8_{-2.0}^{+1.9}$ b/sr, $\bar{a} = -2.43_{-0.17}^{+0.16}$ fm and $\bar{r} = 2.21_{-0.16}^{+0.16}$ fm. But these spin-averaged parameters fail completely to reproduce the total $\Lambda p \rightarrow \Lambda p$ cross section data, see dotted curve in Fig. 3 on the right ($\chi_{red}^2 = 18$). This result indicates that the singlet and triplet effective range parameters are different.

Therefore, we study the missing-mass spectrum and the total Λp cross sections simultaneously in a combined fit. In addition we take a previous measurement of the Λp FSI in the reaction $K^- + d \rightarrow \pi^- + p + \Lambda$ at rest into account

¹ Note the difference of factor 2 in the definition of Φ_3 with respect to [30]

[5] which yielded an independent determination of the triplet parameters, $a_t = -2.0 \pm 0.5$ fm and $r_t = 3.0 \pm 1.0$ fm. These two values and their errors are taken as additional experimental data, i.e. as $1\text{-}\sigma$ constraints for the fitted a_t - and r_t -values in the combined fit. In order to explore the parameter space we start with a five-parameter fit keeping the ratio $|M_t/M_s|^2$ fixed. Starting with $|M_t/M_s|^2 = 1$, we varied the ratio $|M_t/M_s|^2$ between 0 and 8. The resulting χ^2 values depend rather strongly on the ratio $|M_t/M_s|^2$. The optimum fit is achieved with $|M_t/M_s|^2 = 0$. A six-parameter fit confirms this result. The final results are listed in Table 1.

Table 1
Six-parameter fit results.

$ M_s ^2$ (b/sr)	a_s (fm)	r_s (fm)	$ M_t ^2$ (b/sr)	a_t (fm)	r_t (fm)	χ_{red}^2
111_{-38}^{+8}	$-2.43_{-0.25}^{+0.16}$	$2.21_{-0.36}^{+0.16}$	$0.0_{-0.0}^{+19}$	$-1.56_{-0.22}^{+0.19}$	$3.7_{-0.6}^{+0.6}$	0.53

We note that a possible theoretical uncertainty of the Jost-function approach may be in the order of 0.4 fm for the scattering length and even more for the effective range as suggested by the analysis of pseudodata [19]. This aspect will be discussed in a further paper.

Concerning the experimental uncertainties, the overall normalization error yields a systematic error of 10 % for the production matrix element ($|\bar{M}|^2$ and $|M_s|^2$). The effective range parameters are not affected. They depend only on the relative shape of the missing mass spectrum. The scattering length a is mainly determined by the strongly rising part of the spectrum near the Λp threshold. The effective range parameter r depends mainly on the spectral distribution towards higher invariant masses. The relative normalization errors between the three parts of the spectrum yield a systematic error of 0.02 fm for the scattering length (\bar{a} and a_s) and 0.13 fm for the effective range parameter (\bar{r} and r_s). These errors are smaller than the error estimates of the fit, but they must be taken into account in the evaluation of the total error. The precision of the beam momentum and the kaon momenta is so high that the deduced FSI parameters are not affected.

The results shown in Table 1 depend on the accuracy of the included Λp data, especially on the overall normalization of the cross sections, see the right side of Fig. 3. The error bars indicate the statistical errors which are the main source of errors in those hydrogen bubble chamber experiments. The systematic errors are small compared to the statistical errors. The data are based on 378 and 224 elastic Λp scattering events, respectively. They were taken by two independent groups [1,2] using the 81-cm hydrogen bubble chamber at CERN. The two data sets are consistent within the errors.

5 Discussion and conclusion

The reaction $p + p \rightarrow K^+ + (\Lambda p)$ was measured at $T_p = 1.953$ GeV and $\Theta = 0^\circ$ with a high missing mass resolution in order to study the Λp FSI. A three-parameter fit with spin-averaged effective range parameters \bar{a} and \bar{r} yields a good description of the missing mass spectrum but fails completely to describe the momentum dependence of the free Λp scattering. The combined study of the missing mass spectrum and the free Λp scattering using five- and six-parameter fits reveals that the production of the Λp system in the triplet state is rather small. The best fit yields $|M_t|^2 = 0$ and the 1σ limit is reached for $|M_t/M_s|^2 = 0.168$ corresponding to $|M_s|^2 = 73.6$ b/sr and $|M_t|^2 = 12.4$ b/sr. In the fit we take also the independent determination of the triplet parameters a_t and r_t by Tai Ho Tan [5] into account.

It is interesting to note that the spin-averaged parameters \bar{a} and \bar{r} deduced from a three-parameter fit of the missing mass spectrum are identical with the singlet parameters a_s and r_s deduced from a six-parameter fit of both the missing mass spectrum and the free Λp scattering. Also, the fit indicates that the reaction $p+p \rightarrow K^+ + (\Lambda p)$ is dominated by the singlet contribution, however, this result should be considered with respect to the theoretical uncertainties of the Jost-function approach [19]. A direct determination of the singlet and triplet contributions requires polarization measurements as proposed in [18].

The result $|a_s| > |a_t|$ indicates that the Λp interaction is more attractive in the singlet state than in the triplet state. This finding is in accordance with the analysis of the binding energies of light hypernuclei [4]. The present results agree within errors with recent predictions of the new Jülich meson-exchange model J04c [21] yielding $a_s = -2.66$ fm, $r_s = 2.67$ fm, $a_t = -1.57$ fm and $r_t = 3.08$ fm. Recent calculations of the NLO effective field theory yield similar results for a_s , r_s , a_t and r_t [23]. The present results are also in agreement with a similar analysis of the reaction $p + p \rightarrow K^+ + (\Lambda p)$ at $T_p = 2300$ MeV and $\Theta = 10.3^\circ$ [16]. Thus, the method of factorizing the reaction amplitude in terms of a production- and FSI-amplitude yields comparable results for different bombarding energies and scattering angles. In this sense, the present study provides also a systematic check of the method.

We analyze our data using the standard Jost-function approach [17]. The recently proposed dispersion-integral method [18,19] differs from the Jost-function approach by restricting the dispersion integral over the scattering phase shift to a finite upper limit. In a further investigation we will analyze our data using different approaches.

A narrow S=-1 resonance predicted by the cloudy bag model [24] is not visible in our missing mass spectrum. The small structures at 2096.5 ± 1.5 and $2098.0 \pm$

1.5 MeV observed in a previous experiment [11] are not confirmed. Further data analysis is underway in order to quantify the resonance limits. But this is beyond the scope of the present paper.

Acknowledgements

We thank the COSY team for excellent beam preparation. This work was supported by the Bundesministerium für Bildung und Forschung, BMBF (06BN108I), the Forschungszentrum Jülich GmbH, COSY FFE (41520742), the European infrastructure activity under the FP6 'Structuring the European Research Area' programme, contract no. RII3-CT-2004-506078, the Indo-German bilateral agreement and the GAS Slovakia (1/4010/07).

References

- [1] G. Alexander et al., Phys. Rev. **173** (1968) 1452.
- [2] B. Sechi-Zorn et al., Phys. Rev. **175** (1968) 1735.
- [3] R.H. Dalitz, Nucl. Phys. A **354** (1981) 101c.
- [4] C.B. Dover and A. Gal, Prog. Part. Nucl. Phys. **12** (1984) 171.
- [5] Tai Ho Tan, Phys. Rev. Lett. **23** (1969) 395.
- [6] C. Pigot et al., Nucl. Phys. B **249** (1985) 172.
- [7] H. Piekarz, Nucl. Phys. A **479** (1988) 263c.
- [8] A.C. Melissinos et al., Phys. Rev. Lett. **14** (1965) 604.
- [9] J.T. Reed et al., Phys. Rev. **168** (1968) 1495.
- [10] W.J. Hogan, P.A. Piroué and A.J.S. Smith, Phys. Rev. **166** (1968) 1472.
- [11] R. Siebert et al., Nucl. Phys. A **567** (1994) 819.
- [12] J.T. Balewski et al., Eur. Phys. J. A **2**, 99 (1998) 99.
- [13] B. Bilger et al., Phys. Lett. B **420** (1998) 217.
- [14] M. Maggiora et al., Nucl. Phys. A **691** (2001) 329c.
- [15] S. Abd El-Samad et al., Phys. Lett. B **632** (2006) 27.
- [16] F. Hinterberger and A. Sibirtsev, Eur. Phys. J. A **21** (2004) 313.
- [17] M.L. Goldberger and K.M. Watson, *Collision Theory* (J. Wiley, New York, 1964) p. 549.

- [18] A. Gasparyan, et al., Phys. Rev. C **69** (2004) 034006.
- [19] A. Gasparyan, J. Haidenbauer and C. Hanhart, Phys. Rev. C **72** (2005) 034006.
- [20] V.C.J. Stoks and Th.A. Riken, Phys. Rev. C **59** (1999) 3009.
- [21] J. Haidenbauer and U.-G. Meißner, Phys. Rev. C **72** (2005) 044005.
- [22] H. Polinder, J. Haidenbauer and U.G. Meißner, Nucl. Phys. A **779** (2006) 244.
- [23] J. Haidenbauer, Proceedings Few Body Conference, Bonn (2009).
- [24] A.T.M. Aerts and C.B. Dover, Nucl. Phys. B **253** (1985) 116.
- [25] M. Drochner et al., Nucl. Phys. A **643** (1998) 55.
- [26] R. Siudak, et al., Nucl. Instr. and Meth. A **596** (2008) 311.
- [27] D.C. Carey and C. Iselin, TURTLE, A computer program for beam transport simulations including decay, CERN Program Library W151 (1984).
- [28] S. Abdel-Samad, M. Abdel-Bary and K. Kilian Nucl. Instr. and Meth. A **495** (2002) 1.
- [29] V. Bargmann, Rev. Mod. Phys. **21**, 488 (1949).
- [30] A. Sibirtsev et al., Eur. Phys. J. A **32** (2007) 229.